

Bounds on ϵ -rate for Linear, Time-Invariant, Multiinput/Multioutput Channels

DAN HAJELA AND MICHAEL L. HONIG

Abstract—Suppose that a multiinput/multioutput channel is described by a time-invariant, linear operator H , which maps an input vector waveform $u(\cdot)$ to an output vector waveform $y(\cdot)$. The input $u(\cdot)$ is assumed to be bounded in energy (L_2 norm) on the time interval $[0, T]$. Let $N_{\max}(T, \epsilon)$ denote the maximum number of inputs to H for which any pair of distinct outputs are separated by at least ϵ in L_2 norm. The limit of $[\log_2 N_{\max}(T, \epsilon)]/T$ as $T \rightarrow \infty$ is known as “ ϵ -rate.” Here we extend the bounds on ϵ -rate given by Root for single-input/single-output channels to multiinput/multioutput channels. This extension uses a result due to Lerer on the eigenvalue distribution of a convolution operator with a matrix kernel (impulse response). Our results are used to assess the increase in data rate attainable by designing input signals which exploit the multidimensional nature of the channel, relative to treating each constituent channel in isolation. Numerical results based upon a simple model for two coupled twisted-pair wires are presented.

I. INTRODUCTION

GIVEN A COMMUNICATIONS CHANNEL that can be modeled as a multiinput/multioutput (MIMO) time-invariant linear system, we attempt to estimate the maximum data rate that can be reliably communicated in certain situations. In particular, it is assumed that the statistics of any perturbations to the received signal are not easily modeled, so that Shannon theory cannot be applied. The primary motivation for this model is the telephone subscriber loop, which typically consists of twisted-pair wire within a binder group containing many such pairs. The primary channel impairments in this case are crosstalk between wires, typically caused by inductive and capacitive imbalance, and impulse noise. Since crosstalk is a linear effect, however, the entire bundle of wires can be treated as a single linear MIMO channel [4]. If we further assume that coding is used to correct errors due to impulse noise, as proposed in [5], then the remaining thermal noise level due to the wire itself is the primary channel impairment. Since this noise level is quite low, it is anticipated that inaccuracies at the receiver (i.e., imperfect timing recovery, A/D conversion, etc.) will be the dominant cause of transmission errors.

We assume that any perturbations to the received signal caused by the channel and receiver can be modeled by

Manuscript received February 8, 1989; revised March 12, 1990. This work was presented in part at the 1988 Information Theory Symposium, Kobe, Japan, June 1988.

The authors are with Bellcore, 445 South Street, Morristown, NJ 07960-1910.

IEEE Log Number 9036395.

an additive noise process, the statistics of which are unknown, but which is bounded by $\epsilon/2$ in L_2 norm. Two channel outputs are therefore *distinguishable* if they are separated in L_2 norm by ϵ . Let $N_{\max}(T, \epsilon)$ denote the maximum number of distinguishable channel outputs, subject to the constraint that the corresponding inputs are bounded in L_2 norm over the interval $[0, T]$, where $T > 0$. The limit of $[\log_2 N_{\max}(T, \epsilon)]/T$ as $T \rightarrow \infty$ has been called both “ ϵ -rate” and “ ϵ -capacity,” and can be used to estimate the maximum achievable data rate for the situation just described. In this paper we will refer to this quantity as the “ ϵ -rate,” since it has been pointed out to the authors that “ ϵ -capacity” has other meanings in the contexts of both information theory and approximation theory. Upper and lower bounds on ϵ -rate for linear time-invariant single-input/single-output (SISO) channels are given in [1]. Here we extend these results to MIMO channels. In the case of a diagonal $M \times M$ channel transfer matrix with different diagonal entries, we compare the ϵ -rate bounds for the MIMO channel with the sum of the bounds for the constituent SISO channels, assuming that in the latter case input power is allocated so as to maximize the bounds.

The Shannon capacity for a MIMO channel with additive Gaussian noise was derived by Brandenburg and Wyner [3] and was used to estimate the capacity of two coupled twisted-pair wires. The same transfer function model for the two coupled channels considered in [3] is used here to estimate ϵ -rate, and we compare our results with the analogous results from [3]. We also demonstrate the increase in ϵ -rate that can be obtained by treating the coupled channels as a single MIMO channel, rather than as two independent SISO channels. In the latter case, crosstalk between the two channels is treated as noise uncorrelated with the transmitted signals.

Although [1], [6], [8], and [11] are the only references known to the authors that give estimates on ϵ -rate, related work on MIMO channels is given in [3], [4], and [7]. Optimization of transmitter and receiver filters for MIMO channels is studied in [7], and the design of a MIMO communications system for the telephone subscriber loop is discussed in [4]. Bounds on ϵ -rate that hold for a general class of bandpass channels are given in [8].

The next section describes the space of input and output signals in terms of the eigenfunctions and singular values of the channel model. This discussion parallels that

given in [1], with the main distinction being that in our case inputs, outputs, and eigenfunctions are vector-valued rather than scalar-valued. Upper and lower bounds on ϵ -rate for MIMO channels are subsequently given in Sections III and IV, and Section V presents the numerical results.

II. PRELIMINARIES

Let H denote the time-invariant linear operator which models the MIMO channel, and let $\mathbf{H}(\cdot)$ denote the associated complex $M \times M$ matrix impulse response. Let $\mathbf{u}(\cdot)$ be any complex-valued function in $(L_2[0, T])^M$, that is,

$$\|\mathbf{u}\|_T^2 = \sum_{j=1}^M \int_0^T |u_j(s)|^2 ds < \infty \quad (1)$$

where u_j is the j th component of \mathbf{u} . If $\mathbf{u}(\cdot)$ is the input to H , then the output vector $\mathbf{y}(t)$ is given by

$$\mathbf{y}(t) = H[\mathbf{u}](t) = \mathbf{H}^* \mathbf{u}(t) = \int_0^T \mathbf{H}(t-s) \mathbf{u}(s) ds. \quad (2)$$

In addition, we assume that for some $\tau > 0$,

$$h_{ij}(t) = 0, \quad \text{for } t > \tau \text{ and } t < 0 \quad (3a)$$

and

$$h_{ij} \in L_1(-\infty, \infty) \cap L_2(-\infty, \infty) \quad (3b)$$

where $h_{ij} = [\mathbf{H}]_{ij}$, $1 \leq i, j \leq M$. These conditions imply that $\mathbf{y}(t) = 0$ for $t > T + \tau$ and $t < 0$, and that H is a Hilbert-Schmidt operator that maps elements in $(L_2[0, T])^M$ to elements in $(L_2[0, T + \tau])^M$. Let H^* denote the adjoint of H , which maps $(L_2[0, T + \tau])^M$ to $(L_2[0, T])^M$. Then H^*H maps $(L_2[0, T])^M$ to $(L_2[0, T])^M$, and is compact and self-adjoint. It is easily verified that for $\mathbf{u} \in (L_2[0, T])^M$:

$$H^*H[\mathbf{u}](t) = \int_0^T \mathbf{R}(t-s) \mathbf{u}(s) ds \quad (4)$$

where

$$\mathbf{R}(t) = \int_{-\infty}^{\infty} \mathbf{H}^*(s) \mathbf{H}(t+s) ds \quad (5)$$

and \mathbf{H}^* is the conjugate transpose of \mathbf{H} .

In analogy with the SISO case, since $(L_2[0, T])^M$ is a Hilbert space, the spectral theorem can be applied to show that there exists an orthonormal (vector) sequence $\{\phi_j\}$ containing at least one element, where $\phi_j \in (L_2[0, T])^M$ for each j , such that

$$H^*H[\phi_j] = \lambda_j \phi_j, \quad j = 1, 2, \dots \quad (6)$$

where the λ_j are the (scalar) singular values of H and have the following properties: (1) λ_j is real and positive, (2) λ_j has finite multiplicity for each j , and (3) $\lim_{j \rightarrow \infty} \lambda_j = 0$, assuming infinitely many singular values. Furthermore, if we augment the sequence $\{\phi_j\}$ with an orthonormal basis for the null space of H^*H , then the resulting sequence forms a complete orthonormal basis for $(L_2[0, T])^M$. Given any $\mathbf{u} \in (L_2[0, T])^M$, we can therefore

write

$$\mathbf{u}(t) = \sum_{j=1}^{\infty} b_j \phi_j(t) \quad (7)$$

where the scalars $b_j = \langle \mathbf{u}, \phi_j \rangle$ and

$$\|\mathbf{u}\|_T^2 = \sum_{j=1}^{\infty} b_j^2 < \infty. \quad (8)$$

If we let

$$\psi_j = \lambda_j^{-1/2} H[\phi_j] \quad (9)$$

then it is easily verified that $HH^*[\psi_j] = \lambda_j \psi_j$, the ψ_j 's are orthonormal, and that the output \mathbf{y} of H in response to the input given by (7) can be written as

$$\mathbf{y}(t) = \sum_{j=1}^{\infty} \lambda_j^{1/2} b_j \psi_j(t). \quad (10)$$

Let $a_j = \lambda_j^{1/2} b_j$. If we further restrict the inputs to be constrained in energy, i.e., $\|\mathbf{u}\|_T^2 \leq E^2$, then the output space can be represented by the space of real-valued sequences $\{a_j\}$ such that

$$\sum_{j=1}^{\infty} \frac{a_j^2}{\lambda_j} \leq E^2. \quad (11)$$

Because of the properties of λ_j , the output space is therefore a compact ellipsoid with semiaxes $E\lambda_j^{1/2}$.

III. UPPER AND LOWER BOUNDS ON ϵ -RATE

Let $N_{\max}(T, \epsilon)$ denote the maximum number of inputs to H for which any pair of distinct outputs are separated by at least ϵ in L_2 norm, i.e.,

$$N_{\max}(T, \epsilon) = \max \left\{ N: \min_{\substack{i \neq j \\ 1 \leq i, j \leq N}} \|\mathbf{H}^*(\mathbf{u}_i - \mathbf{u}_j)\|_{T+\tau} \geq \epsilon, \right. \\ \left. \|\mathbf{u}_i\|_T^2 \leq E^2, \quad 1 \leq i \leq N \right\}. \quad (12)$$

The ϵ -rate for the channel H is defined as

$$C(\epsilon) = \lim_{T \rightarrow \infty} \frac{\log_2 N_{\max}(T, \epsilon)}{T} \text{ bits/s.} \quad (13)$$

We remark that $N_{\max}(T, \epsilon)$ and $C(\epsilon)$ can be defined using norms other than the L_2 norm [9].

Since the space of output signals can be described by a compact ellipsoid in Hilbert space, the definition (12) can be rewritten as

$$N_{\max}(T, \epsilon) = \max_{a_1, \dots, a_N} \left\{ N: \min_{\substack{i \neq j \\ 1 \leq i, j \leq N}} \|\mathbf{a}_i - \mathbf{a}_j\| \geq \epsilon \right\} \quad (14)$$

where \mathbf{a}_i is the (infinite) vector of coefficients corresponding to $H[\mathbf{u}_i]$, the norm is the Euclidean norm, and the components of \mathbf{a}_i satisfy (11). Upper and lower bounds on $N_{\max}(T, \epsilon)$ in terms of the singular values $\{\lambda_j\}$, based on volume arguments, have been obtained by Root [1]. These bounds ((20) and (22) in [1]) are repeated here for

easy reference,

$$\log_2 N_{\max}(T, \epsilon) \geq \sum_{j=1}^n \log_2 \left(\frac{E\lambda_j^{1/2}}{\epsilon} \right) \quad (15a)$$

and

$$\begin{aligned} \log_2 N_{\max}(T, \epsilon) &\leq \sum_{j=1}^{\bar{n}} \log_2 \left(\frac{2E\lambda_j^{1/2}}{\epsilon} \right) \\ &+ \bar{n} \log_2 \left(\frac{1}{\sqrt{2(1-\alpha^2)}} + \frac{1}{\alpha} \right) \\ &+ \log_2 \left(\frac{\bar{n}+2}{2} \right) \end{aligned} \quad (15b)$$

where α is a constant between zero and one chosen to minimize the upper bound, \bar{n} is the smallest integer for which $\lambda_{\bar{n}}^{1/2} \leq \alpha\epsilon/2E$, and \underline{n} is the largest integer such that $\lambda_{\underline{n}}^{1/2} > \epsilon/E$.

It will also be useful to consider the following approximation to N_{\max} . In particular, we can approximate N_{\max} as the volume of a compact ellipsoid in \mathbf{R}^n containing all possible channel outputs divided by the volume of the sphere in \mathbf{R}^n with radius $\epsilon/2$, where n is chosen to maximize N_{\max} . In particular,

$$N_{\max}(T, \epsilon) \approx \sup_n \frac{\prod_{i=1}^n (E\lambda_i^{1/2})}{(\epsilon/2)^n} = \prod_{i=1}^{\bar{n}} \frac{2E\lambda_i^{1/2}}{\epsilon} \quad (16a)$$

or

$$\log_2 N_{\max}(T, \epsilon) \approx \sum_{i=1}^{\bar{n}} \log_2 \frac{2E\lambda_i^{1/2}}{\epsilon} \quad (16b)$$

where \bar{n} is the largest integer for which $2E\lambda_{\bar{n}}^{1/2} \geq \epsilon$. Note that this approximation is not a bound on $\log_2 N_{\max}$, but lies between the preceding upper and lower bounds.

Since N_{\max} is given by (14) in both the SISO and MIMO cases, the bounds (15) and the approximation (16) must also apply to the MIMO case, where the singular values are defined by (6). To obtain upper and lower bounds for $C(\epsilon)$, given by (13), it is necessary to study the distribution of singular values $\{\lambda_j(T)\}$ as $T \rightarrow \infty$. This has been done by Lerer [2], who proved the following result. Consider the integral equation

$$\int_0^T \mathbf{K}(t-s)\phi(s) ds = \lambda\phi(s) \quad (17)$$

where the Fourier transform of \mathbf{K} , i.e.,

$$\hat{\mathbf{K}}(\omega) = \int_{-\infty}^{\infty} \mathbf{K}(t) e^{-i\omega t} dt,$$

is bounded and absolutely integrable. Denote the eigenvalues of $\hat{\mathbf{K}}(\omega)$ for any fixed ω as $\mu_j[\hat{\mathbf{K}}(\omega)]$, $j=1, 2, \dots, M$. Let G be a compact set that contains the set of eigenvalues

$$\mu_j[\hat{\mathbf{K}}(\omega)], \quad \text{for } j=1, 2, \dots, M \text{ and } -\infty < \omega < \infty$$

and the set of eigenvalues

$$\lambda_j(T), \quad \text{for all } j=1, 2, \dots, \text{ and } 0 < T < \infty.$$

Also, the complement of G must be connected. For any function $\Phi(z)$ defined on the complex z -plane such that $\Phi(z)/z^2$ is continuous and holomorphic on G ,

$$\lim_{T \rightarrow \infty} \frac{\sum_{j=1}^{\infty} \Phi[\lambda_j(T)]}{T} = \frac{1}{2\pi} \int_{-\infty}^{\infty} \sum_{j=1}^M \Phi\{\mu_j[\mathbf{K}(\omega)]\} d\omega. \quad (18)$$

Observe that in the SISO case ($M=1$), \mathbf{K} is a scalar function, and (18) reduces to the well-known Kac-Murdock-Szego theorem [2].

Consider now the case of interest, in which the kernel $\mathbf{K}(t) = \mathbf{R}(t)$, given by (5). Let $\hat{\mathbf{R}}(\omega)$ denote the Fourier transform of $\mathbf{R}(t)$, and let

$$\hat{r}_{ij} = [\hat{\mathbf{R}}]_{ij} = \sum_{k=1}^M \hat{h}_{ik}^* \hat{h}_{kj}.$$

Note that $\hat{r}_{ij}(\omega)$ is bounded, i.e.,

$$\begin{aligned} \sup_{\omega} |\hat{r}_{ij}(\omega)| &\leq \sum_{k=1}^M \left(\sup_{\omega} |\hat{h}_{ik}(\omega)| \right) \left(\sup_{\omega} |\hat{h}_{kj}(\omega)| \right) \\ &\leq \sum_{k=1}^M \left(\int_{-\infty}^{\infty} |h_{ik}(t)| dt \right) \left(\int_{-\infty}^{\infty} |h_{kj}(t)| dt \right) \\ &< J_{ij} < \infty \end{aligned} \quad (19)$$

since $h_{ij} \in L_1(-\infty, \infty)$. Consequently, the eigenvalues $\lambda_j(T)$, defined by (6) with $\mathbf{K} = \mathbf{R}$, are also real and satisfy

$$\lambda_j(T) \leq \sup_{i,k,\omega} |\hat{r}_{ik}(\omega)| < \max_{i,k} J_{ik} \equiv J \quad (20)$$

for each j and for all $T > 0$. Since $\hat{\mathbf{R}}(\omega)$ is positive definite for all ω , its eigenvalues $\mu_j[\hat{\mathbf{R}}(\omega)]$ are real and positive. Furthermore,

$$\begin{aligned} \sup_{i,\omega} \mu_i(\omega) &\leq \sup_{\omega} \text{tr} \hat{\mathbf{R}}(\omega) \\ &\leq M \sup_{i,\omega} |\hat{r}_{ii}(\omega)| < MJ. \end{aligned} \quad (21)$$

Consequently, the set G can be taken to be the interval $[0, MJ]$.

As an example, suppose that $\Phi(x) = \mathcal{D}_{(c,d)}^{\circ}(x)$, the indicator function for the interval (c, d) where $0 < c < d \leq MJ$. Although $\Phi(x)/x^2$ is not continuous on G , we can consider a sequence of functions $\{\Phi_k(x)\}$ such that $\Phi_k(x)/x^2$ is continuous on G for each k , and $\Phi_k(x)$ converges uniformly to $\Phi(x)$ except on a set of measure zero. Applying (18) to $\Phi_k(x)$ and letting $k \rightarrow \infty$ gives

$$\begin{aligned} \lim_{T \rightarrow \infty} \frac{\sum_{j=1}^{\infty} \mathcal{D}_{(c,d)}^{\circ}[\lambda_j(T)]}{T} \\ = \frac{1}{2\pi} \sum_{j=1}^M \text{meas} \{ \omega : c < \mu_j[\hat{\mathbf{R}}(\omega)] < d \} \end{aligned} \quad (22)$$

where "meas S " denotes the Lebesgue measure of the set

S. The numerator in the left-hand side of (22) is simply the number of singular values of the operator H that lie in the interval (c, d) . Loosely speaking, this equation has the following interpretation. In the SISO case each eigenfunction of the linear operator H^*H , ϕ_k , converges to the function $e^{i\omega t}$ for some ω as $T \rightarrow \infty$. The eigenvalue associated with the eigenfunction $e^{i\omega t}$ is $|\hat{h}(\omega)|^2$, where \hat{h} is the Fourier transform of the impulse response. Similarly, in the MIMO case, as $T \rightarrow \infty$, the eigenfunctions of the operator H^*H are vectors whose components are complex exponentials with different amplitudes, i.e., $e^{i\omega t} \mathbf{a}$, where the amplitude vector must satisfy

$$\hat{\mathbf{R}}(\omega) \mathbf{a} = \mu \mathbf{a}, \quad (23)$$

where μ is the associated eigenvalue. Note that if

$$\phi(t) = \sum_{k=1}^M e^{i\omega_k t} \mathbf{a}_k \quad (24)$$

is an eigenfunction of H^*H as $T \rightarrow \infty$, then the associated eigenvalue μ is also an eigenvalue for each term in the sum, $e^{i\omega_k t} \mathbf{a}_k$, where \mathbf{a}_k is a vector of coefficients. Consequently, if all asymptotic eigenfunctions of H^*H have the form (24), then all eigenvalues can be generated, as $T \rightarrow \infty$, by solving (23) for all values of ω .

We now apply Lerer's Theorem to (15a) with

$$\Phi(x) = \log_2 \left(\frac{E\sqrt{x}}{\epsilon} \right) \mathcal{I}_{(\epsilon^2/E^2, \infty)}(x).$$

As in the preceding example, $\Phi(x)$ is not continuous on G ; however, we can again consider a sequence of functions $\{\Phi_k(x)\}$ such that $\Phi_k(x)/x^2$ is continuous on G for each k , and $\Phi_k(x)$ converges uniformly to $\Phi(x)$ except on a set of measure zero. Applying (18) to $\Phi_k(x)$ and letting $k \rightarrow \infty$ gives

$$C(\epsilon) \geq \frac{1}{2\pi} \sum_{j=1}^M \int_{\mu_j(\omega) \geq \epsilon^2/E^2} \log_2 \left(\frac{E\sqrt{\mu_j(\omega)}}{\epsilon} \right) d\omega. \quad (25a)$$

Similarly, we can apply Lerer's theorem to (15b) using continuous approximations to $\Phi(x) = [\log_2(2E\sqrt{x}/\epsilon) + \log_2(1/\sqrt{2(1-\alpha^2)} + 1/\alpha)] \mathcal{I}_{(\alpha^2\epsilon^2/4E^2, \infty)}(x)$. The result is

$$C(\epsilon) \leq \frac{1}{2\pi} \sum_{j=1}^M \int_{\mu_j(\omega) \geq \alpha^2\epsilon^2/4E^2} \left[\log_2 \left(\frac{2E\sqrt{\mu_j(\omega)}}{\epsilon} \right) + \log_2 \left(\frac{1}{\sqrt{2(1-\alpha^2)}} + \frac{1}{\alpha} \right) \right] d\omega. \quad (25b)$$

Note that the right most term in (15b) does not appear in (25b) since \bar{n} increases as $O(T)$, so that for large T ,

$$\frac{1}{T} \log_2 \left(\frac{1}{2} \bar{n} + 1 \right)$$

behaves as $O(\log_2 T/T)$. Finally, we apply Lerer's theo-

rem as in the preceding cases to (16b) to obtain

$$C(\epsilon) \approx \frac{1}{2\pi} \sum_{j=1}^M \int_{\mu_j(\omega) > \epsilon^2/4E^2} \log_2 \left(\frac{2E\sqrt{\mu_j(\omega)}}{\epsilon} \right) d\omega. \quad (26)$$

The bounds and approximation given by (25) and (26) are similar in form to the Shannon capacity of a MIMO additive-white-Gaussian-noise channel with memory (i.e., transfer function $\hat{H}(\omega)$), derived in [3]. In particular, if σ^2 is the spectral density of the noise, then the Shannon capacity for this channel is

$$C_S = \frac{1}{2\pi} \sum_{j=1}^M \int_{\mu_j(\omega) > \sigma^2/K} \log_2 \left(\frac{K\mu_j(\omega)}{\sigma^2} \right)^{1/2} d\omega \quad (27a)$$

where K is chosen to satisfy

$$\frac{1}{2\pi} \sum_{j=1}^M \int_{\mu_j(\omega) > \sigma^2/K} \left(K - \frac{\sigma^2}{\mu_j(\omega)} \right) d\omega = E^2 \quad (27b)$$

where E^2 is the input power, and it is assumed that $\mu_j(\omega) > \sigma^2/K$ holds for ω in a set of finite measure. As an example, consider an SISO additive-white-Gaussian-noise channel with $\hat{H}(\omega) = 1$ for $|\omega| \leq 2\pi W$. In this case the Shannon capacity is

$$C_S = W \log_2 \left(1 + \frac{E^2}{2W\sigma^2} \right). \quad (28)$$

The expected noise power is $\|n\|^2 = 2W\sigma^2$, where $\|f\|^2 = \lim_{T \rightarrow \infty} (1/T) \|f\|_T^2$ for any $f \in L_2$. If we insist that the outputs of $\hat{H}(\omega)$ be pairwise separated by twice the rms value of the noise, i.e., $\epsilon = 2\sqrt{2W\sigma^2}$, then the corresponding ϵ -rate satisfies

$$W \log_2 \frac{E^2}{8W\sigma^2} \leq C(\epsilon) \leq W \left(\log_2 \frac{E^2}{2W\sigma^2} + 2.53 \right) \quad (29)$$

where the value of α in (25b) is taken to be 0.75. We add that it can be shown [11], [12] that $C(\epsilon) \leq C_S$ given by (28) where $\epsilon^2 = 8W\sigma^2$.

IV. EXAMPLE: NO CROSS-COUPLING

For the case of M uncoupled SISO channels we now compare the ϵ -rate of the diagonal $M \times M$ transfer matrix with the sum of the ϵ -rates of the constituent channels. In the latter case we assume that input power is allocated among the channels so as to maximize the upper and lower bounds on $C(\epsilon)$. For an $M \times M$ diagonal transfer matrix, (26) becomes

$$C(\epsilon) \approx \frac{1}{2\pi} \sum_{j=1}^M \int_{B_j} \log_2 \left(\frac{2E\sqrt{\hat{r}_{jj}(\omega)}}{\epsilon} \right) d\omega \quad (30)$$

where

$$\hat{r}_{jj}(\omega) = [\hat{\mathbf{R}}]_{jj} \text{ and } B_j = \left\{ \omega: \hat{r}_{jj}(\omega) \geq \frac{\epsilon^2}{4E^2} \right\}.$$

If the constituent channels are treated independently, then the sum of the ϵ -rates for the constituent channels is

approximately

$$C(\epsilon_1, \dots, \epsilon_M) \approx \frac{1}{2\pi} \sum_{j=1}^M \int_{B_j} \log_2 \left(\frac{2E_j \sqrt{\hat{r}_{jj}(\omega)}}{\epsilon_j} \right) d\omega \quad (31)$$

where in this case

$$B_j = \left\{ \omega: \hat{r}_{jj}(\omega) \geq \frac{\epsilon_j^2}{4E_j^2} \right\}$$

E_j is the rms value of the input to channel j , and the outputs of channel j must be separated by ϵ_j . We can now maximize the right side of (31) with respect to the E_j 's subject to an input energy constraint, i.e., $\sum_{j=1}^M E_j^2 = E^2$. Assuming that

$$\text{meas} \left\{ \omega: \hat{r}_{jj}(\omega) = \frac{\epsilon_j^2}{4E_j^2} \right\} = 0 \quad (32)$$

for each j , then it is easily shown that the solution must satisfy

$$E_j^2 = \frac{E^2 \text{meas } B_j}{\sum_{k=1}^M \text{meas } B_k}, \quad j = 1, \dots, M. \quad (33)$$

For general $\hat{r}_{jj}(\omega)$ this set of equations must be solved numerically. Similarly, if the bounds (25) are maximized with respect to $\{E_j\}$, the solution is again given by (33) with $B_j = \{\omega: \hat{r}_{jj}(\omega) \geq \epsilon_j^2/E_j^2\}$ if the lower bound is maximized, and $B_j = \{\omega: \hat{r}_{jj}(\omega) \geq \alpha^2 \epsilon_j^2/(4E_j^2)\}$ if the upper bound is maximized.

The set of ϵ_j 's in (31) represents the distribution of noise, or receiver inaccuracy, across the constituent SISO channels. Note that the approximations given by (30) and (31) are the same if $E_j/\epsilon_j = E/\epsilon$ for each j . For a fixed distribution of input power, i.e., E_1, \dots, E_M , we can choose the set of ϵ_j 's to minimize the approximation (31) subject to a total noise power constraint, i.e., $\sum_{j=1}^M \epsilon_j^2 = \epsilon^2$. Again, assuming (32) holds for each j , the result is

$$\epsilon_j^2 = \frac{\epsilon^2 \text{meas } B_j}{\sum_{k=1}^M \text{meas } B_k}. \quad (34)$$

Combining (31), (33), and (34) gives the same approximation for $C(\epsilon)$ as (30). For any fixed set of ϵ_j 's, the approximation (31), where the input power is allocated optimally, is therefore always greater than or equal to the approximation (30). This remains true if the bounds (25) are used instead of the approximations for ϵ -rate. Of course, the reason for this is that treating the set of uncoupled SISO channels as one MIMO channel ignores extra information about the distribution of noise across the channels.

In contrast to the preceding discussion, we might instead assume that the receiver can distinguish two signals

(scalar or vector) if and only if they are separated by ϵ in L_2 norm. In this case if the channels are treated independently, then any two distinct outputs of channel j must be separated by $\epsilon_j \geq \epsilon$ for each j . The resulting approximation (31), where E_j is determined by (33), is then always less than or equal to the approximation (30) for the MIMO case. The reason for this is that the minimum separation between two vector outputs must be $\sqrt{M}\epsilon$ if the channels are treated independently, as opposed to a separation of ϵ if the channels are treated as a single MIMO channel.

To illustrate the preceding discussion, consider two uncoupled channels with transfer functions

$$\hat{H}_j(\omega) = \begin{cases} 1, & |\omega| \leq 2\pi W_j \\ 0, & \text{otherwise} \end{cases} \quad j = 1, 2. \quad (35)$$

In this case the approximations (30) and (31) become

$$C(\epsilon) \approx C_1(\epsilon) \equiv 2(W_1 + W_2) \log_2 \frac{2E}{\epsilon} \quad (36)$$

and

$$C(\epsilon_1, \epsilon_2) \approx C_2(\epsilon_1, \epsilon_2) \equiv 2W_1 \log_2 \frac{2E_1}{\epsilon_1} + 2W_2 \log_2 \frac{2E_2}{\epsilon_2}. \quad (37)$$

From (33), the distribution of power that maximizes the approximation (31) is

$$\left(\frac{E_1}{E} \right)^2 = \frac{W_1}{W_1 + W_2} \quad \text{and} \quad \left(\frac{E_2}{E} \right)^2 = \frac{W_2}{W_1 + W_2} \quad (38)$$

independent of ϵ_1 and ϵ_2 , assuming that $\epsilon_j/E_j < 1$, $j = 1, 2$. To compare (36) and (37), we assume that $\epsilon_1^2 = \epsilon_2^2 = \epsilon^2/2$, i.e., that the noise is uniformly distributed across both channels. Combining (37) and (38) gives

$$C_2 \left(\frac{\epsilon}{\sqrt{2}}, \frac{\epsilon}{\sqrt{2}} \right) = C_1(\epsilon) + W_1 \log_2 \frac{2W_1}{W_1 + W_2} + W_2 \log_2 \frac{2W_2}{W_1 + W_2}. \quad (39)$$

It is easily shown that the sum of the last two terms on the right is always nonnegative, which implies that

$$C_1(\epsilon) \leq C_2 \left(\frac{\epsilon}{\sqrt{2}}, \frac{\epsilon}{\sqrt{2}} \right)$$

with equality if and only if $W_1 = W_2$.

The approximations C_1 and C_2 are plotted as a function of $2E/\epsilon$ in Fig. 1 for the case $W_1 = 50$ kHz and $W_2 = 100$ kHz. The corresponding lower and upper bounds obtained from (25) are also shown. The constant α was selected to tighten the upper bound. For the case considered the optimal value of α is approximately 0.75. Also shown in Fig. 1 are upper and lower bounds on ϵ -rate assuming the receiver can distinguish two vector outputs separated by $\epsilon_1 = \epsilon_2 = \epsilon/\sqrt{2}$. In this case the approxima-

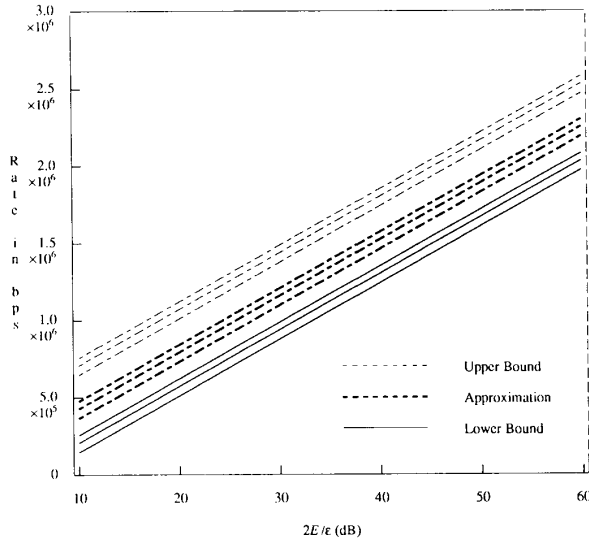


Fig. 1. ϵ -rate vs. $2E/\epsilon$ for transfer function given by (35) assuming: 1) input power is uniformly distributed across both channels, 2) input power is optimally distributed, and 3) receiver can distinguish two channel output vectors separated by ϵ .

tion (30) becomes

$$\begin{aligned} C(\epsilon) &\approx C_3(\epsilon) = 2(W_1 + W_2) \log_2 \frac{2\sqrt{2}E}{\epsilon} \\ &= C_2\left(\frac{\epsilon}{\sqrt{2}}, \frac{\epsilon}{\sqrt{2}}\right) - W_1 \log_2 \frac{W_1}{W_1 + W_2} \\ &\quad - W_2 \log_2 \frac{W_2}{W_1 + W_2}. \end{aligned} \quad (40)$$

It is easily verified that the sum of the last two terms is negative, so that

$$C_2\left(\frac{\epsilon}{\sqrt{2}}, \frac{\epsilon}{\sqrt{2}}\right) \leq C_3(\epsilon).$$

V. NUMERICAL RESULTS

We consider the same model for two coupled twisted-pair wires as was considered in [3] (see also [10]). The transfer matrix is given by

$$\hat{H}(\omega) = e^{-\gamma l} \begin{bmatrix} 1 & ikl^{1/2}\omega \\ ikl^{1/2}\omega & 1 \end{bmatrix} \quad (41)$$

where l is the length of the wire in feet and $\gamma = a\sqrt{\omega} + ib\omega$. The matrix $\hat{R}(\omega) = \hat{H}^*(\omega)\hat{H}(\omega)$ is diagonal with eigenvalues

$$\mu_1(\omega) = \mu_2(\omega) = \mu(\omega) = (1 + \omega^2 k^2 l) e^{-2a/\sqrt{|\omega|}}. \quad (42)$$

Fig. 2 shows a plot of $\mu(\omega)$ for $k = 1.26 \times 10^{-12}$, $a = 0.23 \times 10^{-6}$ (taken from [3]), and $l = 12$ kft. Evaluating the

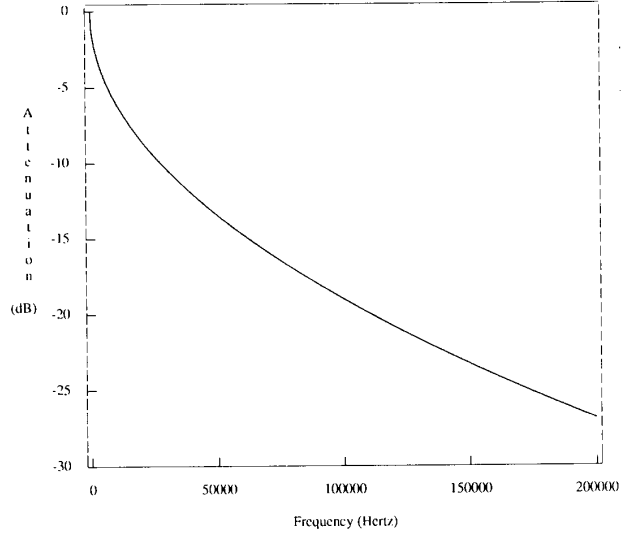


Fig. 2. $\mu(\omega)$ vs. $\omega/(2\pi)$.

bounds (25) gives

$$\begin{aligned} C(\epsilon) &\geq \frac{2}{\pi \ln 2} \left\{ \omega \left(\ln \frac{E}{\epsilon} - 1 \right) - \frac{2al}{3} \omega^{3/2} \right. \\ &\quad \left. + \frac{1}{2} \omega \ln(1 + k^2 l \omega^2) + \frac{1}{kl^{1/2}} \arcsin \frac{kl^{1/2} \omega}{\sqrt{1 + k^2 l \omega^2}} \right\} \end{aligned} \quad (43a)$$

and

$$\begin{aligned} C(\epsilon) &\leq \frac{2}{\pi \ln 2} \left\{ \bar{\omega} \left(\ln \frac{2E}{\epsilon} - 1 \right) - \frac{2al}{3} \bar{\omega}^{3/2} \right. \\ &\quad \left. + \frac{1}{2} \bar{\omega} \ln(1 + k^2 l \bar{\omega}^2) + \frac{1}{kl^{1/2}} \arcsin \frac{kl^{1/2} \bar{\omega}}{\sqrt{1 + k^2 l \bar{\omega}^2}} \right. \\ &\quad \left. + \bar{\omega} \ln \left(\frac{1}{\sqrt{2(1 - \alpha^2)}} + \frac{1}{\alpha} \right) \right\} \end{aligned} \quad (43b)$$

in bits/s where $\mu(\omega) = \epsilon^2/E^2$, and $\mu(\bar{\omega}) = \alpha^2 \epsilon^2/4E^2$. Also, evaluating (26) gives

$$\begin{aligned} C(\epsilon) &\approx \frac{2}{\pi \ln 2} \left\{ \bar{\omega} \left(\ln \frac{2E}{\epsilon} - 1 \right) - \frac{2al}{3} \bar{\omega}^{3/2} \right. \\ &\quad \left. + \frac{1}{2} \bar{\omega} \ln(1 + k^2 l \bar{\omega}^2) + \frac{1}{kl^{1/2}} \arcsin \frac{kl^{1/2} \bar{\omega}}{\sqrt{1 + k^2 l \bar{\omega}^2}} \right\} \end{aligned} \quad (44)$$

where $\mu(\bar{\omega}) = \epsilon^2/(4E^2)$.

Fig. 3 shows plots of the bounds given by (43) and the approximation (44) vs. $2E/\epsilon$ with the same parameters used to generate Fig. 2. It was empirically observed that $\alpha = 0.75$ minimizes the upper bound (43b). Shannon capacity vs. signal-to-noise ratio (SNR), assuming additive white Gaussian noise, is also shown in Fig. 3 for comparison. This curve was computed from (27), assuming that the noise variance, which is the spectral density of the noise σ^2 integrated over the entire channel bandwidth, is

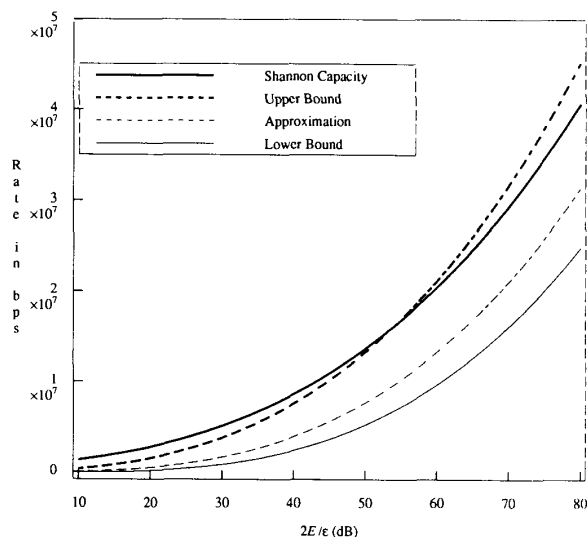


Fig. 3. Bounds on ϵ -rate vs. $2E/\epsilon$ for two coupled twisted pairs 12 kft. in length. Shannon capacity for same cable is also shown.

$\epsilon^2/4$. The SNR in this case therefore corresponds directly to the abscissa of Fig. 3. In all cases the channel bandwidth is assumed to be truncated to the interval $F = \{\omega: 0 \leq \omega \leq 2\pi \times 10^7\}$. The Shannon capacity shown in Fig. 3 is therefore greater than the Shannon capacity computed for the same channel parameters in [3], since the results in [3] assume that the channel bandwidth is truncated to the interval $\hat{F} = \{\omega: 2\pi \times 10^6/2 \leq \omega \leq 2\pi \times 10^7\}$. This assumption was made in [3] because the channel model given by (41) is only accurate in the interval \hat{F} . Clearly, however, the channel frequency response for $0 \leq \omega \leq 2\pi \times 10^6/2$ contributes significantly to both ϵ -rate and Shannon capacity, although relatively speaking this contribution becomes less noticeable at high SNR's, or values of $4E/\epsilon^2$ (i.e., ≥ 60 dB).

Fig. 4 shows bounds and the approximation for ϵ -rate per channel vs. the coupling parameter k for a fixed $2E/\epsilon = 30$ dB. (The corresponding ϵ -rates for the 2×2 channel are twice those shown in Fig. 4.) Also shown in Fig. 4 are bounds on ϵ -rate per channel along with the approximation assuming that the cross-channel coupling, or crosstalk, is treated as additive noise that is uncorrelated with the transmitted signal. In particular, the output of Channel 1 can be written as

$$y_1(t) = h_{11} * u_1(t) + n_X(t) + n_b(t) \quad (45)$$

where $n_X(t) = h_{12} * u_2(t)$ is the noise due to crosstalk, and $n_b(t)$ is the background noise, where it is assumed that $\|n_b\| < \epsilon/2$. Consequently, the L_2 norm of the noise $n_X(t) + n_b(t)$ is upper bounded by

$$\begin{aligned} \frac{\epsilon'}{2} &= \left(\sup_{u_2} \|n_X\|^2 + \frac{\epsilon^2}{4} \right)^{1/2} \\ &= \left(\frac{E^2}{2} \sup_{\omega} |\hat{h}_{12}(\omega)|^2 + \frac{\epsilon^2}{4} \right)^{1/2} \end{aligned} \quad (46)$$

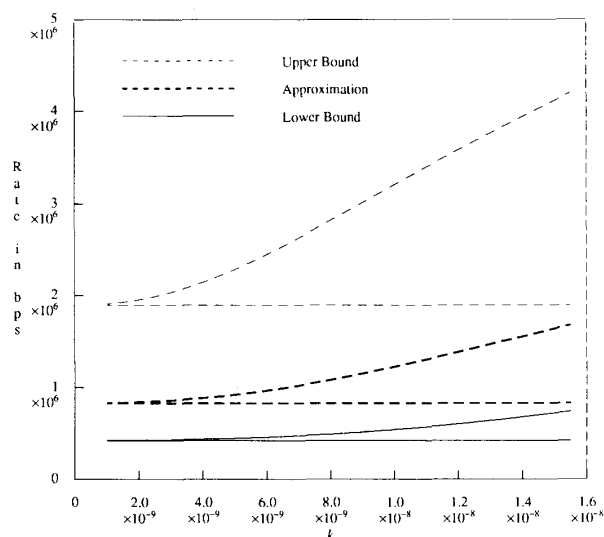


Fig. 4. Bounds on ϵ -rate per channel vs. coupling parameter k for $2E/\epsilon = 30$ dB. Two sets of curves are shown assuming 1) coupled channels are treated as single two-input/two-output channel, and 2) crosstalk between channels is treated as additive noise.

where the last equality assumes that $\|u_2\|^2 \leq E^2/2$. Two outputs of channel 1, with impulse response $h_{11}(t)$, are therefore distinguishable if they are separated by ϵ' . For $\hat{H}(\omega)$ given by (41), $\sup_{\omega} |\hat{h}_{12}(\omega)|$ occurs at $\omega = (2/al)^2$, so that

$$\frac{\epsilon'}{2} = \left(\frac{2E^2k^2}{la^2e^4} + \frac{\epsilon^2}{4} \right)^{1/2}. \quad (47)$$

If the channels are treated independently, then the ϵ -rate of both channels is given by the sum of the ϵ -rates for each SISO channel, where ϵ is replaced by ϵ' . The lower set of curves shown in Fig. 4 therefore converge to zero as k becomes large. Note that if k is fixed, and if $2E/\epsilon \rightarrow \infty$, then the effective SNR, $4E^2/\epsilon'^2$, converges to the constant $la^2e^4/2k^2$, so that the upper and lower bounds on ϵ -rates converge to constants. In contrast, if the two channels are treated as one two-input/two-output channel, then the ϵ -rates increase with k . This is due to the fact that the channel output energy corresponding to any particular input increases with k .

Fig. 5 shows approximate ϵ -rates per channel given by (44) vs. $2E/\epsilon$ with cable length as a parameter. (A "cable" in this case refers to the two-input/two-output channel.) It is shown in the appendix that for both large and small $2E/\epsilon$,

$$C(\epsilon) \approx \frac{2}{3a^2l^2\pi \ln 2} \left(\ln \frac{2E}{\epsilon} \right)^3. \quad (48)$$

In particular, $C(\epsilon)$ increases as the cube of $\log_2(2E/\epsilon)$, and is inversely proportional to the square of the cable length.

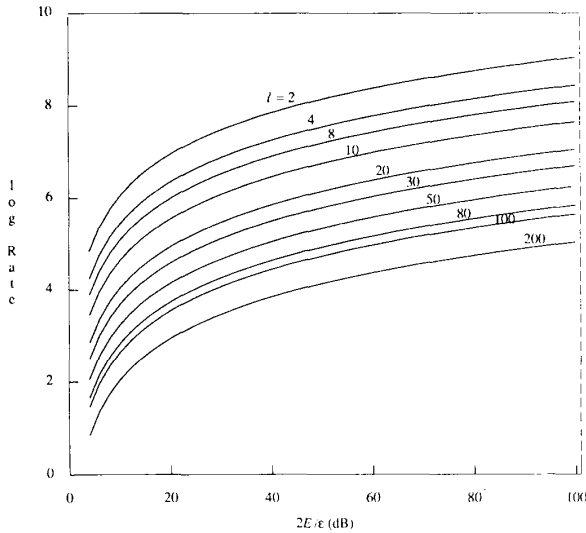


Fig. 5. Approximations to ϵ -rate per channel vs. $2E/\epsilon$ with cable length (in thousands of feet) as parameter.

The results in Fig. 5 indicate that for the channel model considered, and for a desired rate of 1.0×10^6 bits/s, the ratio of input power to output separation E/ϵ should be approximately 45 dB for a 20-kft cable, and approximately 20 dB for a 10-kft cable. The previous analysis assumes, however, that transmission over the cable occurs in only one direction at a time (half-duplex). In the case of simultaneous transmission in both directions (full-duplex), near-end crosstalk must also be taken into account [4], [10].

It is interesting to note that the behavior of ϵ -rate for large and small $2E/\epsilon$, as given by (48), is qualitatively different from the behavior of Shannon capacity for the same channel transfer function with additive Gaussian noise. In particular, it is shown in [3] that the Shannon capacity and cable length are linearly related for high SNR's, and are logarithmically related for small SNR's. In contrast, ϵ -rate is inversely proportional to cable length squared for large $2E/\epsilon$. In addition, Shannon capacity becomes a linear function of SNR as the SNR becomes large, and is a logarithmic function of SNR for small SNR, whereas ϵ -rate varies asymptotically as the cube of $\log_2 2E/\epsilon$.

VI. CONCLUSION

Upper and lower bounds on the ϵ -rate of a linear, time-invariant MIMO channel have been derived by using the same volume argument previously used by Root [1] for SISO channels. Because these bounds are not very tight, we have also presented an approximation to the ϵ -rate, which lies between the upper and lower bounds, and can be used to compare ϵ -rates for different channels. We add that the upper bound presented here can be improved upon [12].

The motivating application for this work is communication in a multitwisted-pair environment in which crosstalk between twisted-pairs is a major channel impairment. The preceding bounds have been used to quantify the increase in ϵ -rate that can be obtained by treating two coupled twisted-pairs as a two-input/two-output channel, rather than as two independent SISO channels. In the latter case, the crosstalk has been modeled as additive noise with unknown statistics. As shown in Fig. 4, the difference in ϵ -rates for these two situations increases dramatically as the coupling constant k increases above the threshold of approximately 3×10^{-9} .

We have also considered the problem of allocating input power among M uncoupled SISO channels so as to maximize the ϵ -rate. The form of the optimal distribution, given by (33), depends on the set of receiver discriminations, ϵ_j , $j = 1, \dots, M$, and each SISO channel transfer function. This solution may be applicable to the situation in which the total input power to a MIMO channel is constrained, and the transmitter cannot coordinate the signals on each constituent SISO channel.

A comparison between the ϵ -rate and Shannon capacity has also been given for a model of two coupled twisted-pairs. The Shannon capacity was computed assuming an additive white Gaussian noise with variance $\epsilon^2/4$. The approximation to ϵ -rate was found to be significantly less than the Shannon capacity. The reason for this is that the ϵ -rate assumes no statistical description of the noise, and therefore gives an estimate of maximum channel throughput that must apply to an entire class of noisy channels, as opposed to the Shannon capacity computed here, which specifically applies to the additive white Gaussian noise channel. Further comparisons of Shannon capacity and ϵ -rate are given in [11] and [12].

In the case of full-duplex transmission over multiple twisted-pairs, one of the major channel impairments is near-end crosstalk [4], [10], which typically cannot be modeled as additive Gaussian noise. Assuming that this crosstalk interference is bounded in L_2 norm by ϵ , then the ϵ -rate can be used as an alternative to Shannon capacity for estimating maximum channel throughput in this situation.

ACKNOWLEDGMENT

The authors thank B. Gopinath and Kenneth Steiglitz for helpful discussions concerning this work.

APPENDIX

BEHAVIOR OF ϵ -RATE FOR LARGE AND SMALL $2E/\epsilon$

We first consider the case of large $2E/\epsilon$, and study the behavior of the approximate formula (44). It is easily verified that (48) remains true if either the upper or lower bounds given in (43) are used instead. Since $\mu(\omega)$, defined by (42), is a monotonically decreasing function of ω for large enough ω , $\bar{\omega} \rightarrow \infty$ as $2E/\epsilon \rightarrow \infty$, where $\mu(\bar{\omega}) = \epsilon^2/4E^2$. For very large

$2E/\epsilon$, the approximation (44) therefore becomes

$$C(\epsilon) \approx \frac{2}{\pi \ln 2} \left(\bar{\omega} \ln \frac{2E}{\epsilon} - \frac{2al}{3} \bar{\omega}^{3/2} + \frac{1}{2} \bar{\omega} \ln \bar{\omega}^2 \right) \quad (49)$$

where terms proportional to $\bar{\omega}$ have been discarded. Now (42) implies that

$$\mu(\bar{\omega}) \approx \bar{\omega}^2 k^2 l e^{-2al\sqrt{\bar{\omega}}} = \frac{\epsilon^2}{4E^2} \quad (50)$$

so that as $\bar{\omega} \rightarrow \infty$,

$$\ln \bar{\omega} - al\sqrt{\bar{\omega}} = \ln \frac{\epsilon}{2E} \quad (51)$$

or

$$\sqrt{\bar{\omega}} \approx \frac{1}{al} \ln \frac{2E}{\epsilon}. \quad (52)$$

Substituting (52) into (49) gives

$$\begin{aligned} C(\epsilon) &\approx \frac{2}{3a^2 l^2 \pi \ln 2} \left(\ln \frac{2E}{\epsilon} \right)^3 \\ &\quad + \frac{4}{a^2 l^2 \pi \ln 2} \left(\ln \frac{2E}{\epsilon} \right)^2 \left(\ln \left[\ln \frac{2E}{\epsilon} \right] - \ln al \right) \\ &\approx \frac{2}{3a^2 l^2 \pi \ln 2} \left(\ln \frac{2E}{\epsilon} \right)^3 \end{aligned} \quad (53)$$

for very large $2E/\epsilon$.

We now study the behavior of the approximation (44) when $2E/\epsilon > 1$ and $2E/\epsilon \approx 1$. From the definition of $\bar{\omega}$ and (42), it follows that $\bar{\omega} \approx 0$. Consequently,

$$\frac{2E}{\epsilon} \approx e^{al\sqrt{\bar{\omega}}} \quad (54)$$

and (44) can therefore be approximated as

$$\begin{aligned} C(\epsilon) &\approx \frac{2}{\pi \ln 2} \left[\bar{\omega} (al\sqrt{\bar{\omega}} - 1) - \frac{2al}{3} \bar{\omega}^{3/2} \right. \\ &\quad \left. + \frac{1}{2} \bar{\omega} \left(k^2 l \bar{\omega}^2 - \frac{1}{2} k^4 l^2 \bar{\omega}^4 \right) + \frac{1}{kl^{1/2}} \arcsin kl^{1/2} \bar{\omega} \right] \end{aligned}$$

$$\begin{aligned} &\approx \frac{2}{\pi \ln 2} \left[al\bar{\omega}^{3/2} - \bar{\omega} - \frac{2al}{3} \bar{\omega}^{3/2} + \frac{1}{2} k^2 l \bar{\omega}^3 - \frac{1}{4} k^4 l^2 \bar{\omega}^5 \right. \\ &\quad \left. + \frac{1}{kl^{1/2}} \left(kl^{1/2} \bar{\omega} + \frac{k^3 l^{3/2}}{6} \bar{\omega}^3 \right) \right] \\ &\approx \frac{2}{\pi \ln 2} \left(al\bar{\omega}^{3/2} - \bar{\omega} - \frac{2al}{3} \bar{\omega}^{3/2} + \bar{\omega} \right) \\ &= \frac{2al}{3\pi \ln 2} \bar{\omega}^{3/2} \end{aligned} \quad (55)$$

where the approximations

$$\ln(1+x) \approx x - \frac{1}{2}x^2 \quad \text{and} \quad \arcsin x \approx x + \frac{1}{6}x^3$$

for $x \approx 0$ have been used. Combining (54) and (55) gives (48). It is easily verified that if $E/\epsilon > 1$ and $E/\epsilon \approx 1$, then the lower bound on ϵ -rate given by (43a) can also be approximated by (48) where $2E$ is replaced by E . The upper bound on $C(\epsilon)$, given by (43b), exhibits different behavior for small $2E/\epsilon$ since the last term on the right-hand side of (43b) becomes dominant as $\bar{\omega} \rightarrow 0$.

REFERENCES

- [1] W. L. Root, "Estimates of ϵ capacity for certain linear communication channels," *IEEE Trans. Inform. Theory*, vol. IT-14, no. 3, pp. 361-369, May 1968.
- [2] L. E. Lerer, "On approximating the spectrum of convolutional-type operators, 1. Wiener-Hopf Matricial Integral Operators," *Israeli J. Math.*, vol. 30, no. 4, pp. 339-362, 1978.
- [3] L. H. Brandenburg and A. D. Wyner, "Capacity of the Gaussian channel with memory: The multivariate case," *B.S.T.J.*, vol. 53, no. 5, pp. 745-778, May-June 1974.
- [4] M. Honig, K. Steiglitz, and B. Gopinath, "Multi-channel signal processing for data communications in the presence of crosstalk," *IEEE Trans. Commun.*, vol. 38, no. 4, pp. 551-558, Apr. 1990.
- [5] J. W. Modestino, D. H. Sargrad, and R. E. Bollen, "Use of coding to combat impulse noise on digital subscriber loops," *IEEE Trans. Commun.*, vol. 36, no. 5, pp. 529-537, May 1988.
- [6] R. T. Prosser and W. L. Root, "The ϵ -entropy and ϵ -capacity of certain time-invariant channels," *J. Math. Anal. Applic.*, vol. 21, pp. 233-241, 1968.
- [7] J. Salz, "Digital transmission over cross-coupled linear channels," *B.S.T.J.*, vol. 64, no. 6, pp. 1147-59, July-Aug. 1985.
- [8] A. D. Wyner, "A bound on the number of distinguishable functions which are time-limited and approximately band-limited," *SIAM J. Applied Math.*, vol. 24, no. 3, pp. 289-297, May 1973.
- [9] D. J. Hajela and M. L. Honig, "On finding maximally separated signals for digital communications," in *Open Problems in Communication and Computation*. New York: Springer-Verlag, 1987, pp. 92-99.
- [10] H. Cravis and T. V. Crater, "Engineering of T1 carrier system repeated lines," *B.S.T.J.*, vol. 42, no. 2, pp. 431-486, Mar. 1983.
- [11] L. J. Forsy and P. P. Varaiya, "The ϵ -capacity of classes of unknown channels," *Inform. Contr.*, vol. 14, pp. 376-406, 1969.
- [12] M. L. Honig and P. Narayan, "A new upper bound on ϵ -capacity," *Int. Symp. Inform. Theory*, San Diego, CA, Jan. 14-19, 1990.